IRSTI 29.19 https://doi.org/10.26577/RCPh.2022.v81.i2.011

A. Houbi[1*], Y. Atassi[2], A.A. Zharmenov[1], Zh.T. Bagasharova[1],
S.K. Myrzalieva[1], K.B. Kadyrakunov[3], B.A. Karibayev

[1]The Institute of Complex Processing of Mineral Raw Materials, Kazakhstan, Almaty
[2]The Institute Higher Institute for Applied Sciences and Technology, Syria, Damascus
[3]Engineering Technological University, Kazakhstan, Almaty
[4]Al-Farabi Kazakh National University, Kazakhstan, Almaty
*email: Anashoubi@gmail.com

MICROWAVE ABSORPTION AND ELECTROMAGNETIC INTERFERENCE SHIELDING PROPERTIES OF CARBON BLACK/MnNiZn FERRITE NANOCOMPOSITES-FILLED PARAFFIN WAX IN THE FREQUENCY RANGE (8.8–12 GHz)

In this present work, we offer the design of good, wideband microwave absorption materials (MAMs) based on CB/$Mn_{0.1}Ni_{0.5}Zn_{0.4}Fe_2O_4$ (carbon black/MnNiZn ferrite). The ferrite is prepared by a self-combustion method using sucrose as fuel. The chemical is utilized for the synthesis of carbon black nanopowder is carbon black powder (2–8 µm). Then, the operation is continued via mixing carbon black and MnNiZn ferrite through the grinding balls. Four various weight ratios of CB/$Mn_{0.1}Ni_{0.5}Zn_{0.4}Fe_2O_4$ (1:0, 1:1, 2:1, and 3:1) with various thicknesses (2–4–6 mm) are prepared. X-ray diffractometry and FTIR spectroscopy are utilized in order to characterize samples. The morphology of the powders is investigated by SEM. The electromagnetic interference (EMI) shielding and microwave absorption properties are measured in the frequency band of 8.8–12 GHz to accomplish the practical characterization. The MAMs show broad bandwidths under -10 dB in the range of 0.3–3.2 GHz and reasonable surface density in the range of 2.91–3.66 kg/m^2 with a weight ratio within a paraffin matrix of 40% w/w. The MAM shows a minimal reflection loss of -18.3 dB at the frequency of 11.4 GHz for the thickness of 2 mm. The maximum shielding efficiency is 18.5 dB at 11.5 GHz for 2 mm thickness of the CB/F-21 nanocomposite sample.

Key words: MnNiZn ferrite, carbon black, Absorption bandwidth, Reflection loss, Shielding efficiency.

А. Хуби[1*], И. Атасси[2], А.А. Жарменов[1], Ж. Т. Багашарова[1],
С.К. Мырзалиева[1], К.Б. Кадыракунов[3], Б.А. Карибаев[4]
[1]Институт комплексной переработки минерального сырья, Казахстан, г. Алматы
[2]Высший институт прикладных наук и технологий, Сирия, г.Дамаск
[3]Казахстанский инженерно-технологический университет, Казахстан, г. Алматы
[4]Казахский национальный университет им. аль-Фараби, Казахстан, г. Алматы
*e-mail: Anashoubi@gmail.com

Свойства поглощения микроволн и экранирования электромагнитных помех нанокомпозитов черного углерода/феррит MnNiZn с парафиновым наполнителем в диапазоне 8,8–12 ГГц

В данной работе нами предложена разработка материалов с широкополосным поглощением микроволнового излучения на основе CB/$Mn_{0.1}Ni_{0.5}Zn_{0.4}Fe_2O_4$ (черный углерод/феррит MnNiZn). Ферриты получены методом самовозгорания с использованием сахарозы в качестве топлива. Химикат используется для синтеза нанопорошка, представляющего собой порошок сажи (2–8 мкм). Затем операцию продолжают путем перемешивания сажи и феррита MnNiZn через мелющие шары. Готовят четыре различных весовых соотношения CB/$Mn_{0.1}Ni_{0.5}Zn_{0.4}Fe_2O_4$ (1:0, 1:1, 2:1 и 3:1) различной толщины (2, 4, 6 мм). Рентгеновская дифрактометрия и FTIR-спектроскопия используются для определения характеристик образцов. Морфологию порошков исследуют с помощью СЭМ. Экранирование электромагнитных помех (ЭМП) и свойства поглощения микроволн измеряются в полосе частот 8,8–12 ГГц для получения практических характеристик. Материалы, поглощающие микроволновое излучение, имеют широкую полосу пропускания ниже -10 дБ в диапазоне 0,3–3,2 ГГц и приемлемую поверхностную плотность в диапазоне 2,91–3,66 кг/м2 при весовом соотношении в парафиновой матрице 40% по весу. Материал, поглощающий микроволновое излучение, при толщине 2 мм демонстрирует минимальное значение обратной потери (-18,3 дБ) на частоте 11,4 ГГц. Максимальная эффективность экранирования составляет 18,5 дБ на частоте 11,5 ГГц для образца нанокомпозита CB/F-21 толщиной 2 мм.

Ключевые слова: Феррит MnNiZn, черный углерод, полоса поглощения, обратные потери, эффективность экранирования.

А. Хуби[1*], И. Атасси[2], А.А. Жарменов[1], Ж. Т. Бағашарова[1], С.К. Мырзалиева[1], К.Б. Қадыракунов[3], Б.А. Кәрібаев[4]

[1]Минералды шикізатты кешенді өңдеу институты, Қазақстан, Алматы қ.

[2]Қолданбалы ғылымдар және технологиялар жоғары институты, Сирия, Дамаск қ.

[3]Қазақстан инженерлік-технологиялық университеті, Қазақстан, Алматы қ.

[4]Әл-Фараби атындағы Қазақ ұлттық университеті, Қазақстан, Алматы қ.

*e-mail: Anashoubi@gmail.com

Парафинмен толтырылған қара көміртекті/MnNiZn ферритті нанокомпозиттердің 8,8-12 ГГц диапазонындағы микротолқынды жұтылу және электромагниттік экрандау қасиеттері

Бұл жұмыста CB/$Mn_{0.1}Ni_{0.5}Zn_{0.4}Fe_2O_4$ (қара көміртек /MnNiZn ферриті) негізіндегі кең жолақты микротолқынды сіңіру материалдарының жасалынуы ұсынылған. Ферриттер сахарозаны отын ретінде қолдану арқылы өздігінен жану арқылы алынады. Химиялық зат көміртекті қара ұнтақ (2–8 мкм) болып табылатын наноұнтақ синтезі үшін қолданылады. Операция содан кейін ұнтақтау шарлары арқылы қара көміртекті және MnNiZn ферритін араластыру арқылы жалғасады. Әртүрлі қалыңдықтағы (2, 4, 6 мм) CB/$Mn_{0.1}Ni_{0.5}Zn_{0.4}Fe_2O_4$ (1:0, 1:1, 2:1 және 3:1) төрт түрлі салмақ қатынасы дайындалады. Үлгілерді сипаттау үшін рентгендік дифракция және FTIR спектроскопиясы қолданылады. Ұнтақтардың морфологиясы SEM көмегімен зерттеледі. Практическалық сипаттамаларды алу үшін электромагниттік кедергілерді (EMI) қорғау және микротолқынды жұту қасиеттері 8,8-12 ГГц жиілік диапазонында өлшенді. Микротолқынды жұтатын материалдар 0,3-3,2 ГГц диапазонында -10 дБ-ден төмен кең өткізу қабілеттілігіне және салмағы бойынша 40% парафиндік матрицадағы салмақ қатынасында 2,91-3,66 кг/$м^2$ диапазонында қолайлы аумақтық тығыздыққа ие. Микротолқынды жұтатын материал қалыңдығы 2 мм болатын 11,4 ГГц жиілікте -18,3 дБ кері шағылуын көрсетеді. Қалыңдығы 2 мм CB/F-21 нанокомпозиттік үлгісі үшін экрандаудың максималды тиімділігі 11,5 ГГц жиілікте 18,5 дБ-ді құрайды.

Түйін сөздер: MnNiZn ферриті, қара көміртегі, сіңіру жолағы, кері шағылу, экрандау тиімділігі.

Introduction

The current development of electronics and intelligent devices wide the world has generated electromagnetic interference (EMI), which is currently becoming a critical problem in the microwave frequency bands [1–6]. Repression of EMI and EM radiation plays an essential part in beating this critical problem. Materials that can reduce EMI draw a lot of notice due to their important part in blocking undesirable EMI. Presently, several dielectric loss materials such as conductive polymers and carbon materials or magnetic loss materials such as metal oxides have played an essential role in elevated-frequency EM wave absorption. Nevertheless, the defects involving elevated density, low reflection absorption, and narrow wideband have hugely limited conventional loss materials' workable benefits for EM wave absorption [7–10]. Recently, MA composites based on carbon and ferrite, have obtained significant concern due to their excellent electrical and ferrimagnetic characteristics. Carbonaceous materials-based composites have pulled in major attention for microwave absorption lately such as carbon nanotubes, carbon fibers, graphene and carbon black because of the unique structure of carbon-based materials. More precisely, carbon black is usually used to fit the requirements of high-effective microwave attenuation materials because of its superior characteristics, for example, high permittivity, high specified surface region, unique electronic conductivity, huge interface, etc. [11,12]. Carbon black has a unique place in the range of elevated-frequency MAMs. Furthermore, spinel ferrites have excellent MA characteristics due to their unique magnetic characteristics. MnNiZn ferrites are considered suitable materials for high-frequency implementations [13,14]. When MnNiZn ferrite is blended with CB, the MA characteristics of the resultant composite are anticipated to enhance. According to this, CB/$Zn_{0.8}Ni_{0.2}Fe_2O_4$ nanoparticles scattered in a SiO_2 matrix were successfully synthesized by Anh et al. [15]. The effects of $Zn_{0.8}Ni_{0.2}Fe_2O_4$ nanoparticles range (0–1.75 wt%) and various coating thicknesses (1–2.5 mm) on MA performance in the X-band frequency have been investigated. The outcomes indicated that a specimen of 1.5 wt% $Zn_{0.8}Ni_{0.2}Fe_2O_4$ nanoparticles content showed the highest MA at 10 GHz frequency. Higher coating thicknesses (1–2.5 mm) showed bigger MA and arrived at a so high absorption of 2 mm thickness. On the other hand, Akhtar et al. [16] designed strontium ferrite epoxy (SrF) nanocomposite and CB-loaded CBSrF nanocomposite. The minimum reflection loss (RL_{min}) for the SrF nanocomposite is -25.19 dB at 13.32 GHz for 10.5 mm thickness, whereas for CBSrF nanocomposite the RL_{min} is -31.15 dB at 10.32 GHz for 9.5 mm thickness. Therefore, the CB-loaded SrF nanocomposite exhibits higher attenuation effectiveness than the SrF nanocomposite. In the present work, we study the effect of different weight ratios of CB/$Mn_{0.1}Ni_{0.5}Zn_{0.4}Fe_2O_4$ and its effect on EMI shielding and MA properties. The aim of the study is to prepare MAMs that have high shielding effectiveness and wideband absorbers with a weight ratio within a paraffin matrix of 40% w/w and bandwidth that covers almost the whole frequency band (8.8–12 GHz). The experimental operation consists of synthesizing the ferrite by a self-combustion method. After that, the operation is continuous by mixing and grinding CB and MnNiZn ferrite by the grinding balls.

Methods and materials

Synthesis of ferrite ($Mn_{0.1}Ni_{0.5}Zn_{0.4}Fe_2O_4$) nanoparticles

Ferrite ($Mn_{0.1}Ni_{0.5}Zn_{0.4}Fe_2O_4$) nanoparticles were prepared by a self-combustion method. $Mn_{0.1}Ni_{0.5}Zn_{0.4}Fe_2O_4$ were synthesized by taking appropriate amounts of nickel (II) nitrate hexahydrate ($Ni(NO_3)_2{\cdot}6H_2O$), zinc nitrate hexahydrate ($Zn(NO_3)_2{\cdot}6H_2O$), iron(III) nitrate nonahydrate ($Fe(NO_3)_3.9H_2O$) and manganese(II) chloride tetrahydrate ($MnCl_2$ $.4H_2O$) were blended together with an aqueous solution of sucrose (2 moles per metal ion) and 2% an aqueous solution of polyvinyl alcohol (PVA). The whole mixture was blended totally and heated at 90 °C for 7 h to shape a viscous liquid. The heating process was accompanied by the evolution of brown fumes of NO_2 from the decomposed metal nitrate salts. After that, the mixture was transferred to dry for 2 h at 200 °C in the furnace to obtain a fluffy carbonaceous pyrolyzed mass. After that, the resulting mass was annealed at 750 °C for 4 h to obtain nanoparticles of ferrite.

Preparation of carbon black nanopowder

The average particle size of as-extradited carbon black powder was measured utilizing the sieve shaker and it was between 2–8 μm. Carbon black nanopowder has been created via the grinding balls. The as-extradited carbon black powder was milled for 12 h at 300 rpm.

Preparation of CB/$Mn_{0.1}Ni_{0.5}Zn_{0.4}Fe_2O_4$ nanocomposites

CB nanopowder and ferrite nanoparticles were mixed and milled by the grinding balls. Four various weight ratios of CB/$Mn_{0.1}Ni_{0.5}Zn_{0.4}Fe_2O_4$ (1:0, 1:1, 2:1, and 3:1) were prepared. The CB/$Mn_{0.1}Ni_{0.5}Zn_{0.4}Fe_2O_4$ nanocomposites were ball-milled for 1 h at 300 rpm. Table 1 shows the symbols of nanocomposite samples.

Synthesis of samples for measuring the MA and EMI shielding properties

Paraffin wax was symmetrically blended with CB/$Mn_{0.1}Ni_{0.5}Zn_{0.4}Fe_2O_4$ nanocomposites powders with a weight ratio of nanocomposites within a paraffin matrix of 40% w/w by heating and stirring for 15 min. Thereafter, the absorption samples with various thicknesses (2–4–6 mm) were molded to measure RL and shielding efficiency (SE) in the frequency band (8.8–12 GHz).

Results and discussion

XRD patterns

The crystalline structures of the nanopowders are defined by XRD. The XRD patterns of $Mn_{0.1}Ni_{0.5}Zn_{0.4}Fe_2O_4$ and CB nanopowders are shown in Figure 1. For the $Mn_{0.1}Ni_{0.5}Zn_{0.4}Fe_2O_4$ pattern, six diffraction peaks are noticed, which conform to (hkl) planes of (220), (311), (400), (422), (511) and (440), respectively. The ideal spinel structure is noticed by the peaks of MnNiZn ferrite [17]. The XRD pattern of $Mn_{0.1}Ni_{0.5}Zn_{0.4}Fe_2O_4$ is totally matched with the reference XRD patterns (JCPDS, PDF no. 08–0234). On the other hand, for the CB pattern, two diffraction peaks are noticed, which conform to (hkl) planes of (002) and (100), respectively [18].

Table 1 – Symbols of nanocomposite samples.

Sample symbols	Weight ratio	
	Carbon black	$Mn_{0.1}Ni_{0.5}Zn_{0.4}Fe_2O_4$
CB/F-10	1	0
CB/F-11	1	1
CB/F-21	2	1
CB/F-31	3	1

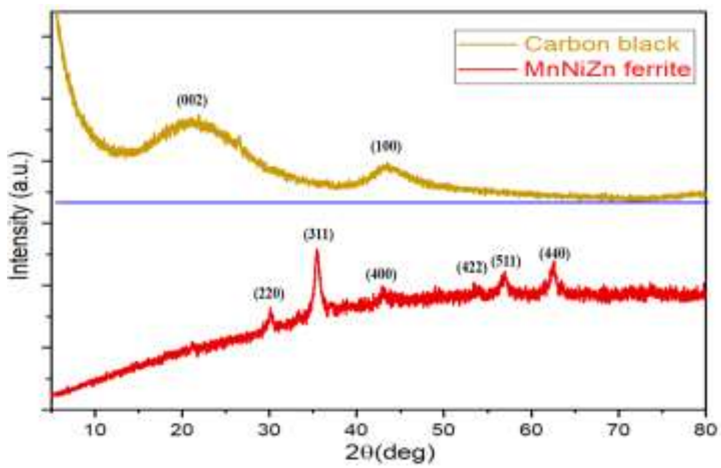

Figure 1 - XRD patterns of MnNiZn ferrite and carbon black.

FTIR spectra

Figure 2 shows the FTIR spectra of the $Mn_{0.1}Ni_{0.5}Zn_{0.4}Fe_2O_4$ nanoparticles and CB nanopowder. For the $Mn_{0.1}Ni_{0.5}Zn_{0.4}Fe_2O_4$ nanoparticles, two peaks at 571.6 cm^{-1} and 446.3 cm^{-1} are referring to the stretching vibration of (Fe-O), which emphasizes the forming of the metal-oxygen in ferrite-based [19]. On the other hand, the peak at 1630.4 cm^{-1} in $Mn_{0.1}Ni_{0.5}Zn_{0.4}Fe_2O_4$ and CB is referring to C=O stretching vibration, and the peaks at 2348 cm^{-1} and 3452 cm^{-1} are referring to O-H stretching vibration [20,21].

SEM analysis

The morphology of the MnNiZn ferrite and CB is verified by SEM, which is illustrated in Figure 3. In Figure 3 (a), one can notice the agglomerated spherical particles of MnNiZn ferrite. The average diameters of the spherical-shaped particles are observed to be ranging between 21–59 nm. On the other hand, the average particle size of CB nanopowder (Figure 3 (b)) is noticed to be ranging between 75–481 nm.

EMI shielding and MA properties

There are two general methods that cope with the interference of incident electromagnetic waves: the first one is electromagnetic interference (EMI) shielding and the second one is microwave absorption (MA). For the EMI shielding method (Figure 4a), the significant point is to attenuate the transmitted power of the EM waves (p_T). On the other hand, for the microwave absorption method (Figure 4b), though, a metal plate is put to reflect the transmitted power of the EM waves. As a consequence, the transmitted power of the EM waves is negligible in microwave absorption. EMI shielding and MA properties of the prepared samples are estimated with the free-space technique. EM waves are generated by a microwave generator in the frequency band of 8.8–12 GHz (with wavelengths λ= 2.5-3.4 cm), where a microwave generator is connected by a WR90 waveguide instrument (IEC Standard R100, X Band). The incident EM waves (p_{in}) are measured by the horn antenna connected to an oscilloscope, then the prepared sample perpendicularly is placed between a microwave generator and the horn antenna to measure the transmitted power of the EM waves (p_T) by an oscilloscope. As a result, SE can be calculated for the EMI shielding by applying the equation (1) [22]:

$$SE\ (dB) = SE_R + SE_A + SE_M = 10\ log\frac{p_{in}}{p_T}. \quad (1)$$

It is significant to note that the multiple reflection loss (SE_M) can be ignored if the absorption shielding (SE_A) of EMI shielding material is higher than 10 dB and equation (1) then can be rewritten as [22]:

$$SE\ (dB) = SE_R + SE_A = 10\ log\frac{p_{in}}{p_T}. \quad (2)$$

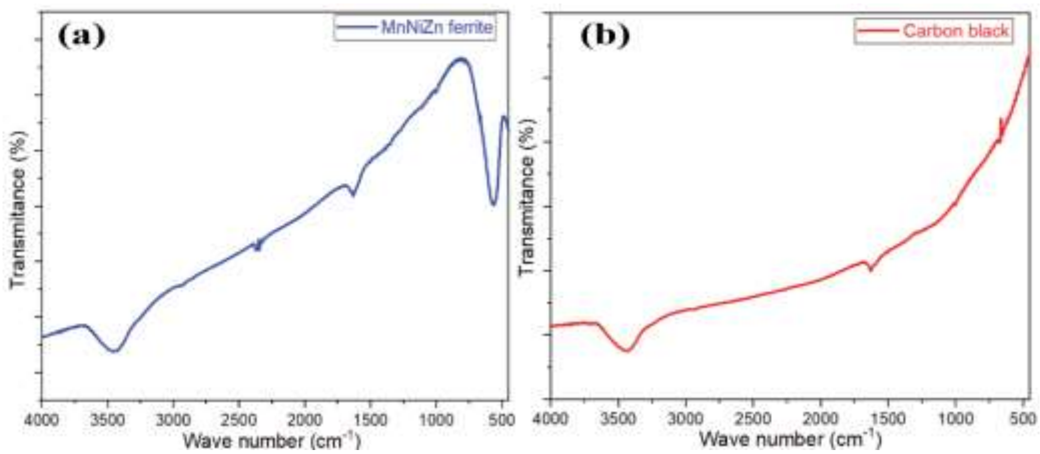

Figure 2 - FTIR spectra of (a) MnNiZn ferrite and (b) carbon black.

In addition to that, the reflected power of the EM waves (p_{ref}) is measured when the EM waves are incident on the sample surface at an angle of 45° by an oscilloscope. As a result, the shielding by reflection (SE_R) can be calculated for the EMI shielding by applying the equation (3).

$$SE_R\ (dB) = -10\log(1-R) = = -10\log\left(1-\frac{p_{ref}}{p_{in}}\right). \quad (3)$$

Finally, the shielding by absorption (SE_A) is calculated by equation (4) [23,24]:

$$SE_A\ (dB) = -10\log\left(\frac{T}{1-R}\right) = = -10\log\left(\frac{p_T}{p_{in}-p_{ref}}\right). \quad (4)$$

Figure 5 represents the shielding efficiency (SE) of CB/$Mn_{0.1}Ni_{0.5}Zn_{0.4}Fe_2O_4$ nanocomposites in the frequency band (8.8–12 GHz) with various thicknesses (2–4–6 mm). The results illustrate that the maximum shielding efficiency is 18.5 dB at the frequency of 11.5 GHz for the thickness of 2 mm of the CB/F-21 nanocomposite sample. Figure 6 shows the SE_R and SE_A of CB/$Mn_{0.1}Ni_{0.5}Zn_{0.4}Fe_2O_4$ nanocomposites with various thicknesses (2–4–6 mm) at the frequency of 11.5 GHz. For the microwave absorption method, the prepared sample is placed on the metal plate at an angle of 45° to measure the reflected power of the EM waves (p_{ref}) by an oscilloscope. As a result, RL can be calculated by applying the equation (5) [23,24]:

$$Rl\ (dB) = 10log\frac{p_{in}}{p_{ref}}. \quad (5)$$

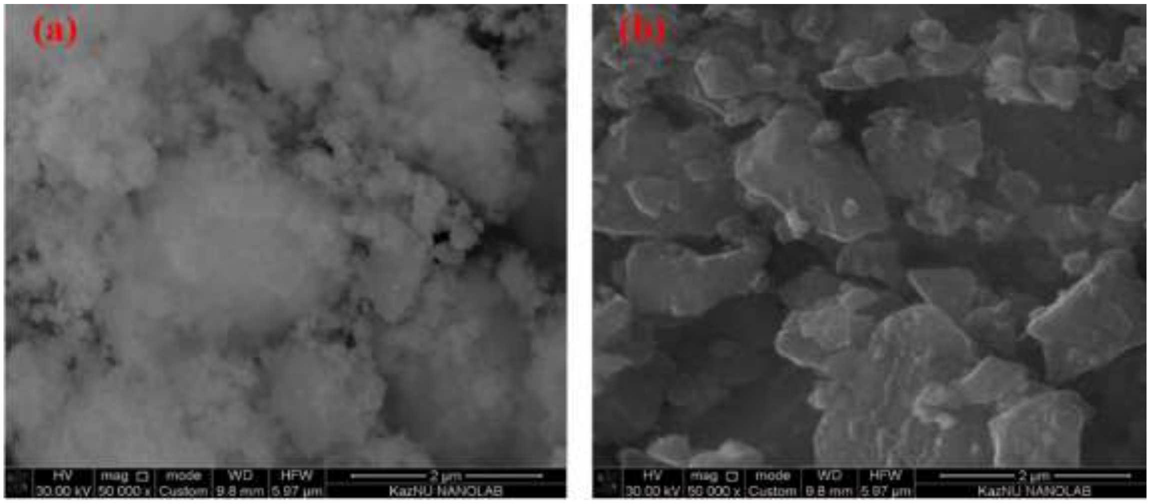

Figure 3 - SEM images of (a) MnNiZn ferrite and (b) carbon black

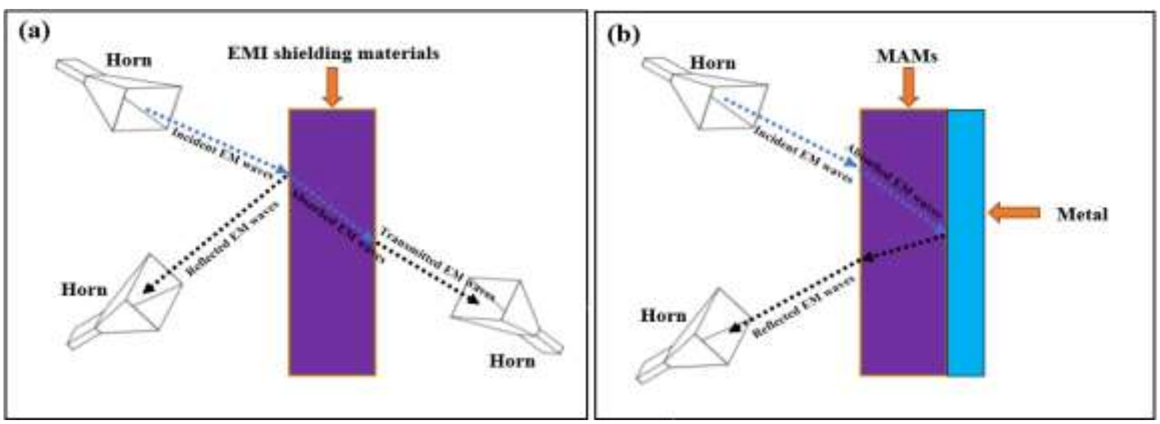

Figure 4 - Sketch of the estimate models of (a) electromagnetic interference shielding and (b) microwave absorption.

Figure 7 illustrates the RL of CB/$Mn_{0.1}Ni_{0.5}Zn_{0.4}Fe_2O_4$ nanocomposites with various thicknesses (2–4–6 mm) at the weight percentage of the absorber within a paraffin matrix (40% w/w). Figure 7 illustrates that the RL attenuation peaks of samples moved to lower frequencies with increasing sample thickness. This phenomenon may be defined by the quarter-wavelength (λ/4) cancellation model, as shown in equation (6) [25–27]:

$$t_m = \frac{c}{4tf_m\sqrt{|\mu_r||\varepsilon_r|}}. \qquad (6)$$

Where $|\varepsilon_r|$ and $|\mu_r|$ are the modulus of the measured complex relative permittivity (ε_r) and permeability (μ_r) at matching frequency (f_m), respectively. c is the velocity of light.

Table 2 shows the low surface density (SD) of all the prepared absorbers. As a result, one can notice the impact of incorporating $Mn_{0.1}Ni_{0.5}Zn_{0.4}Fe_2O_4$ (magnetic loss material) and CB (dielectric loss material) on the EMI and MA properties of the prepared absorber. This incorporation drives to an effective and low thickness absorber with a wide bandwidths under -10 dB (BW_{-10dB}) [28].

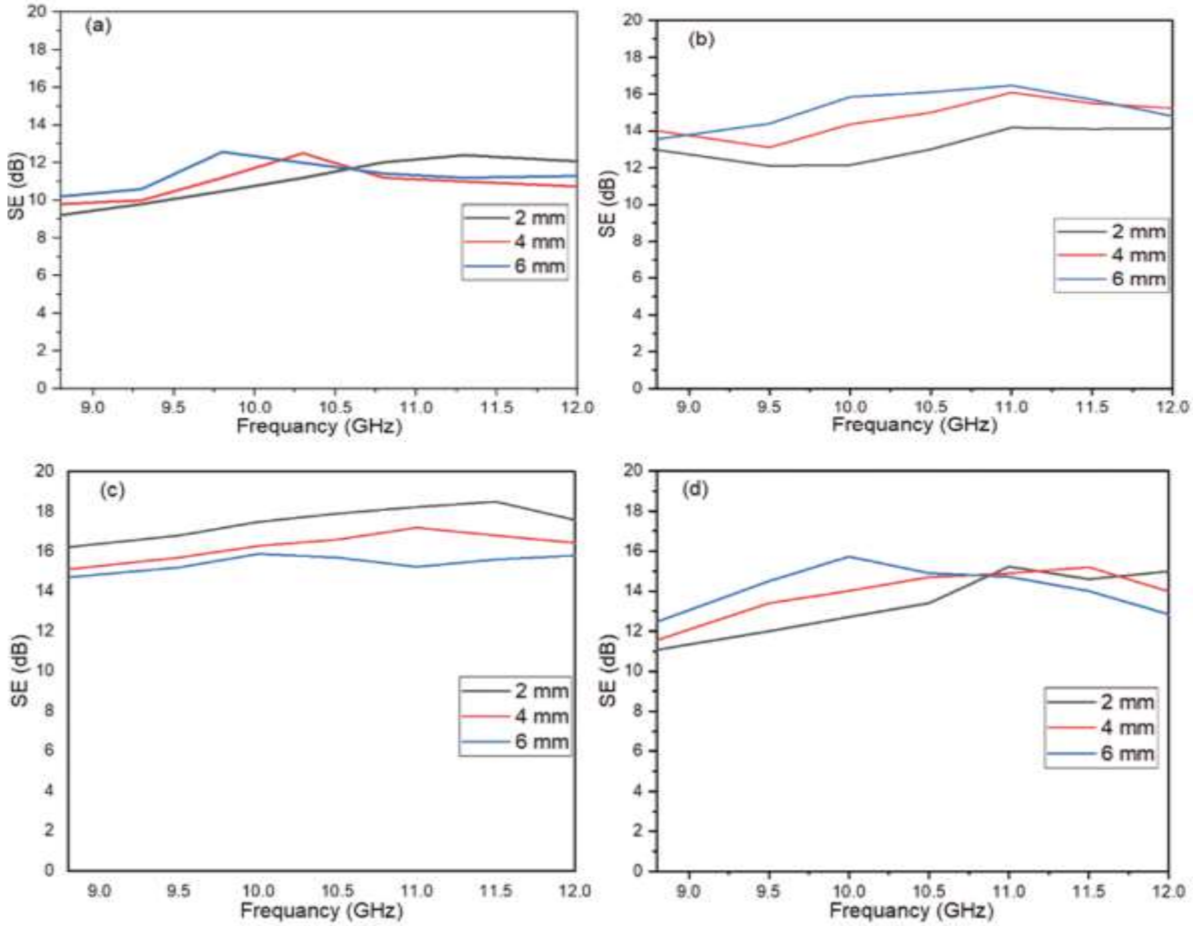

Figure 5 − SE curves of (a) CB/F-10 nanocomposite, (b) CB/F-11 nanocomposite, (c) CB/F-21 nanocomposite and (d) CB/F-31 nanocomposite at various thicknesses (2–4–6 mm).

Table 2 – MA behavior of CB/$Mn_{0.1}Ni_{0.5}Zn_{0.4}Fe_2O_4$ nanocomposites at various thicknesses (2–4–6 mm).

Nanocomposite samples	t (mm)	RL_{min} (dB)	f_m (GHz)	$BW_{-10\ dB}$ (GHz)	SD (kg/m^2)	$BW_{-10\ dB}$/SD (GHz.m^2/kg)
CB/F-10	2	-11.6	10.9	0.7	2.91	0.24
	4	-12.5	10.4	0.8	2.92	0.27
	6	-11.3	9.8	0.3	2.94	0.10
CB/F-11	2	-14.7	11.5	2.0	3.63	0.55
	4	-15.8	11.0	3.2	3.65	0.88
	6	-13.9	10.1	2.9	3.66	0.79
CB/F-21	2	-18.3	11.4	3.2	3.40	0.94
	4	-17.2	10.5	3.2	3.41	0.94
	6	-17.1	10.0	2.8	3.43	0.82
CB/F-31	2	-15.1	11.0	2.5	3.09	0.81
	4	-14.6	10.6	2.9	3.11	0.93
	6	-16.7	9.9	2.6	3.12	0.83

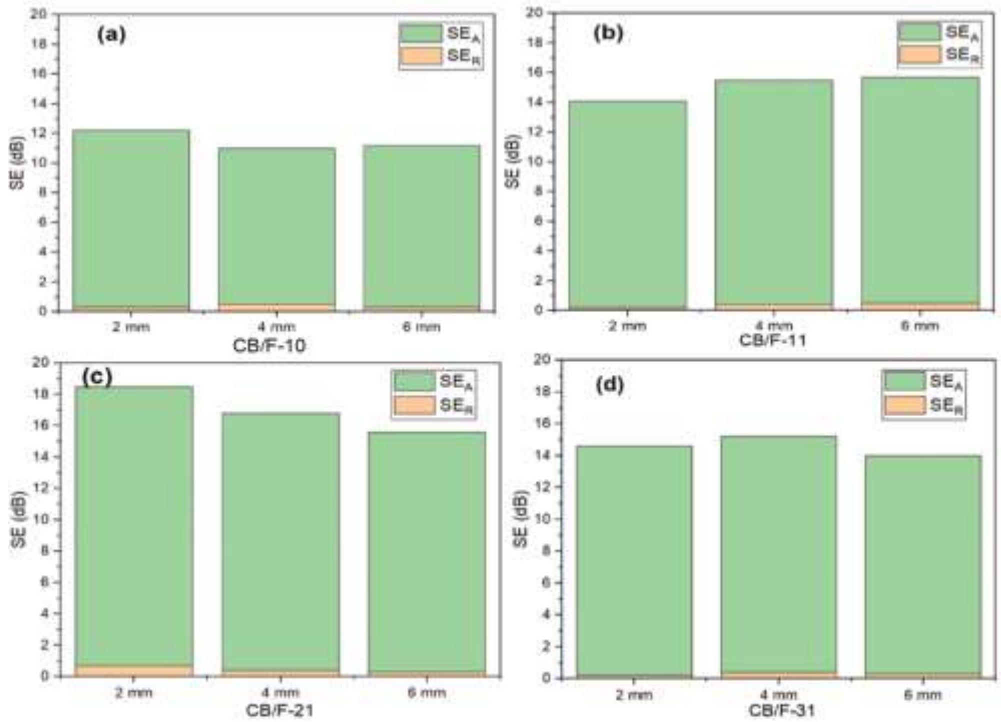

Figure 6 – Bar plot for individual components of SE_R and SE_A of (a) CB/F-10 nanocomposite, (b) CB/F-11 nanocomposite, (c) CB/F-21 nanocomposite and (d) CB/F-31 nanocomposite with various thicknesses (2–4–6 mm) at the frequency of 11.5 GHz.

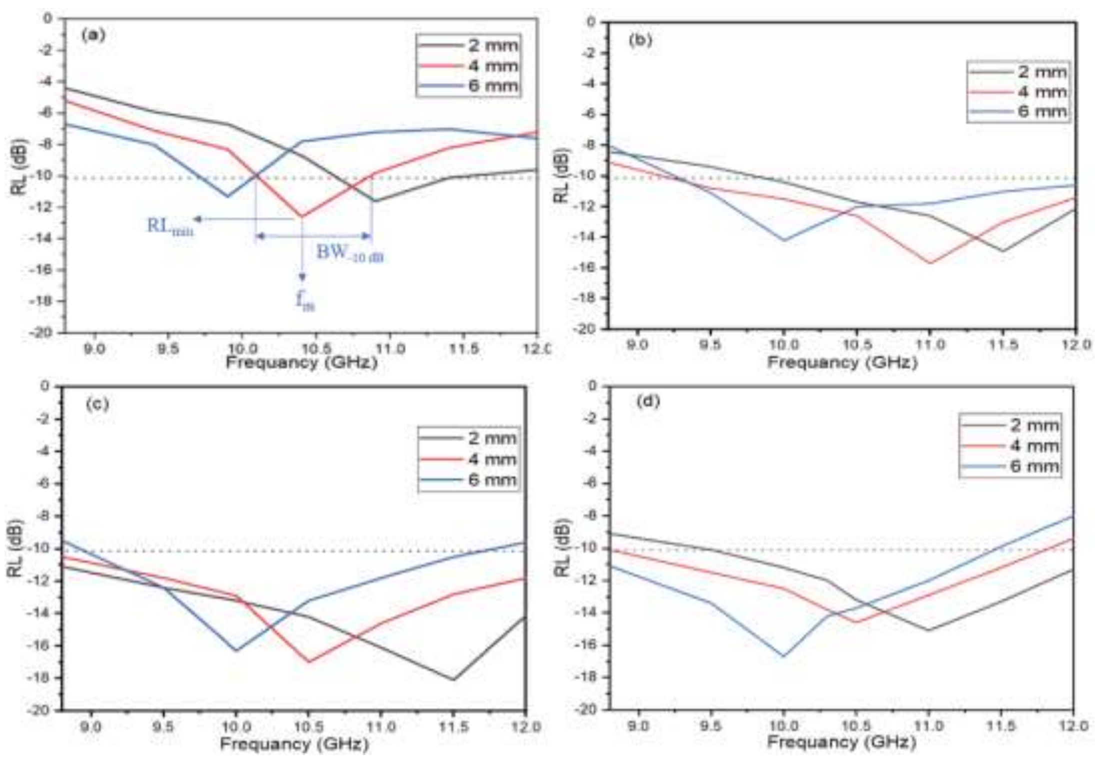

Figure 7 – RL curves of (a) CB/F-10 nanocomposite, (b) CB/F-11 nanocomposite, (c) CB/F-21 nanocomposite, and (d) CB/F-31 nanocomposite at various thicknesses (2–4–6 mm).

Conclusions

In this work, a unique type of lightweight microwave absorber was prepared by using a combination of CB/$Mn_{0.1}Ni_{0.5}Zn_{0.4}Fe_2O_4$ within a paraffin matrix. CB was introduced to enhance the mechanism of dielectric loss, while $Mn_{0.1}Ni_{0.5}Zn_{0.4}Fe_2O_4$ was used to enhance the mechanism of magnetic loss. As a result, one can notice the impact of combining $Mn_{0.1}Ni_{0.5}Zn_{0.4}Fe_2O_4$ and CB on the EMI and MA properties of the absorber. This combination drives to an effective and low thickness microwave absorber with a wide BW_{-10dB}. The results indicate that the RL_{min} of the absorber is -18.3 dB at 11.4 GHz and the absorption BW_{-10dB} is 3.2 GHz for 2 mm thickness and its SD doesn't surpass 3.66 kg/m^2. The maximum SE is 18.5 dB at 11.5 GHz for mm thickness of the CB/F-21 nanocomposite sample.

Acknowledgements

The authors express their gratitude to Al-Farabi Kazakh National University, the center of complex processing of mineral raw materials, and the center of physical-chemical methods of research and analyses for providing the materials and equipment to achieve this research project.

References

1 Lv H., Yang Z., Ong SJH., Wei C., Liao H., Xi S., et al. A Flexible Microwave Shield with Tunable Frequency-Transmission and Electromagnetic Compatibility. //Adv Funct Mater. – 2019. – Vol.29. – P.1-8.

2 Liang C., Qiu H., Song P., Shi X., Kong J., Gu J. Ultra-light MXene aerogel/wood-derived porous carbon composites with wall-like "mortar/brick" structures for electromagnetic interference shielding. //Sci Bull [Internet]. Science China Press. – 2020. – Vol.65. – P.616-622.

3 Chen X., Shi T., Zhong K., Wu G., Lu Y. Capacitive behavior of MoS2 decorated with FeS2@carbon nanospheres. //Chem Eng J. – 2020. – Vol.379. – Art.No 122240.

4 Chen S., Meng G., Kong B., Xiao B., Wang Z., Jing Z., et al. Asymmetric alicyclic amine-polyether amine molecular chain structure for improved energy storage density of high-temperature crosslinked polymer capacitor. //Chem Eng J. – 2020. – Vol.387, May. – Art.No.123662.

5 Cheng C., Chen Z., Huang Z., Zhang C., Tusiime R., Zhou J., et al. Simultaneously improving mode I and mode II fracture toughness of the carbon fiber/epoxy composite laminates via interleaved with uniformly aligned PES fiber webs. //Compos Part A Appl Sci Manuf. – 2020. – Vol.129. – ArtNo.105696.

6 Xu H., Yin X., Li X., Li M., Liang S., Zhang L., et al. Lightweight Ti 2 CT x MXene/Poly(vinyl alcohol) Composite Foams for Electromagnetic Wave Shielding with Absorption-Dominated Feature. //ACS Appl Mater Interfaces. American Chemical Society. – 2019/ - Vol.11. – P.10198-207.

7 Liu Y., Liu X., Wang X. Synthesis and microwave absorption properties of Ni-Zn-Mn spinel ferrites. //Adv Appl Ceram. – 2015. – Vol.114. – P.82-86.

8 Ari Adi W., Yunasfi Y., Mashadi M., Sahidin Winatapura D., Mulyawan A., Sarwanto Y., et al. Metamaterial: Smart Magnetic Material for Microwave Absorbing Material //In book Electromagnenic Fields and Waves, 2019. – P.1-18.

9 Liu P.J., Yao Z.J., Ng V.M.H., Zhou J.T., Yang Z.H., Kong L.B. Enhanced microwave absorption properties of double-layer absorbers based on spherical NiO and Co0.2Ni0.4Zn0.4Fe2O4 ferrite composites. //Acta Metall Sin (English Lett. The Chinese Society for Metals). – 2018. – Vol.31. – P.171-180.

10 Indrusiak T., Pereira I.M., Heitmann A.P., Silva J.G., Denadai Â.M.L., Soares B.G. Epoxy/ferrite nanocomposites as microwave absorber materials: effect of multilayered structure. //J Mater Sci: Mater Electron. – 2020. – Vol.31. – P.13118-13130.

11 Mondal K., Balasubramaniam B., Gupta A., Lahcen A.A., Kwiatkowski M. Carbon Nanostructures for Energy and Sensing Applications. /J Nanotechnol. – 2019. – Vol.2019. – P.10-12.

12 Kwiatkowski M., Policicchio A., Seredych M., Bandosz T.J. Evaluation of CO2 interactions with S-doped nanoporous carbon and its composites with a reduced GO: Effect of surface features on an apparent physical adsorption mechanism. //Carbon N Y. – 2016. – Vol.98. – P.250-257.

13 Ting T.H., Yu R.P., Jau Y.N. Synthesis and microwave absorption characteristics of polyaniline/NiZn ferrite composites in 2-40 GHz. //Mater Chem Phys. – 2011. – Vol.126. – P.364-370.

14 Houbi A., Zharmenov A.A., Atassi Y., Bagasharova Z.T., Mirzalieva S., Kadyrakunov K. Microwave absorbing properties of ferrites and their composites: A review. // J Magn Magn Mater. – 2021. – Vol.529. – Art.No.167839.

15 Anh L.T.Q., Van Dan N. A microwave-absorbing property of super-paramagnetic zinc–nickel ferrite nanoparticles in the frequency range of 8–12 GHz. //Appl Phys A Mater Sci Process. – 2020. – Vol.126. – P.1-6.

16 Chakradhary V.K. and Akhtar M.J. Microwave absorption properties of strontium ferrite and carbon black based

nanocomposites for stealth applications //2017 IEEE Asia Pacific Microwave Conference (APMC). – 2017. – P.678-681.

17 El Nahrawy A.M., El-Deen H.S., Soliman A.A., Mosa W.M.M. Crystallographic and magnetic properties of Al3+co-doped NiZnFe2O4 nano-particles prepared by sol-gel process. //Egypt J Chem. – 2019. – Vol.62. – P.925-957.

18 Hu E., Hu X., Liu T., Fang L., Dearn K.D., Xu H. The role of soot particles in the tribological behavior of engine lubricating oils //Wear. – 2013. – Vol.304. – P.152-161.

19 Kondawar S.B., Nandapure A.I. Magnetic and electrical properties of zinc-substituted nickel ferrite reinforced conducting polyaniline nanocomposites. //J Chinese Adv Mater Soc. – 2014. – Vol.2. – P.186-198.

20 Figueroa Ramírez S.J., Miranda-Hernánde M. Carbon film electrodes as support of metallic particles. //Int J Electrochem Sci. – 2012. – Vol.7. – P.150-166.

21 Kim S.Y., Kwon S.H., Liu Y.D., Lee J.S., You C.Y., Choi H.J. Core-shell-structured cross-linked poly(glycidyl methacrylate)-coated carbonyl iron microspheres and their magnetorheology. //J Mater Sci. – 2014. – Vol.49. –P.1345-1352.

22 Verma P., Bansala T., Chauhan S.S., Kumar D., Deveci S., Kumar S. Electromagnetic interference shielding performance of carbon nanostructure reinforced, 3D printed polymer composites. //J Mater Sci. – 2021. – Vol.56. – P.11769-11788.

23 Bayat M., Yang H., Ko F.K., Michelson D., Mei A. Electromagnetic interference shielding effectiveness of hybrid multifunctional Fe_3O_4/carbon nanofiber composite. //Polymer (Guildf). – 2014. – Vol.55. – P.936-943.

24 Hong Y.K., Lee C.Y., Jeong C.K., Lee D.E., Kim K., Joo J. Method and apparatus to measure electromagnetic interference shielding efficiency and its shielding characteristics in broadband frequency ranges. //Rev Sci Instrum. – 2003. – Vol.74. – P.1098.

25 Wang S., Jiao Q., Shi Q., Zhu H., Feng T., Lu Q., et al. Synthesis of porous nitrogen-doped graphene decorated by γ-Fe2O3 nanorings for enhancing microwave absorbing performance. //Ceram Int. – 2020. – Vol.46. – P.1002-1010.

26 Shu R., Zhang J., Guo C., Wu Y., Wan Z., Shi J., et al. Facile synthesis of nitrogen-doped reduced graphene oxide/nickel-zinc ferrite composites as high-performance microwave absorbers in the X-band. //Chem Eng J. – 2020. – Vol.384. – Art.No123266.

27 Jaiswal R., Agarwal K., Kumar R., Kumar R., Mukhopadhyay K., Prasad N.E. EMI and microwave absorbing efficiency of polyaniline-functionalized reduced graphene oxide/γ-Fe2O3/epoxy nanocomposite. //Soft Matter. – 2020. – Vol.16. – P.6643-6653.

28 Ali N.N., Atassi Y., Salloum A., Malki A., Jafarian M., Almarjeh R.K.B. Lightweight broadband microwave absorbers of core–shell (polypyrrole/NiZn ferrite) nanocomposites in the X-band: insights on interfacial polarization. //J Mater Sci Mater Electron. – 2019. – Vol.30. – P.6876-6887.

References

1 H. Lv, Z. Yang, S.J. H. Ong, C. Wei, H. Liao, S.Xi, Y. Du, G. Ji, and Z.J. Xu, Adv. Funct. Mater., 29, 1-8 (2019).

2 C. Liang, H. Qiu, P. Song, X. Shi, J. Kong, and J. Gu Sci., Bull., 65, 616-622 (2020).

3 X. Chen, T. Shi, K. Zhong, G. Wu, and Y. Lu, Chem. Eng. J, 379, 122240 (2020).

4 S. Chen, G. Meng, B. Kong, B. Xiao, Z. Wang, Z. Jing, Y. Gao, G. Wu, H. Wang, and Y. Cheng, Chem. Eng. J, 387, 123662 (2020).

5 C. Cheng, Z. Chen, Z. Huang, C. Zhang, R. Tusiime, J. Zhou, Z. Sun, Y. Liu, M. Yu, and H. Zhang, Compos. Part A Appl. Sci. Manuf., 129, 105696 (2020).

6 H. Xu, X. Yin, X. Li, M. Li, S. Liang, L. Zhang, and L. Cheng, ACS Appl. Mater. Interfaces 11, 10198 (2019).

7 Y. Liu, X. Liu, and X. Wang, Adv. Appl. Ceram., 114, 82-86 (2015).

8 W. Ari Adi, Y. Yunasfi, M. Mashadi, D. Sahidin Winatapura, A. Mulyawan, Y. Sarwanto, Y. Edi Gunanto, and Y. Taryana, Electromagn Fields Waves, 1-18 (2019).

9 P.J. Liu, Z.J. Yao, V.M. H. Ng, J.T. Zhou, Z.H. Yang, and L.B. Kong, //Acta Metall. Sin. (English Lett. The Chinese Society for Metals), 31, 171-180 (2018).

10 T. Indrusiak, I.M. Pereira, A.P. Heitmann, J.G. Silva, Â.M.L. Denadai, and B.G. Soares //J. Mater. Sci. Mater. Electron., 31, 13118-13130 (2020).

11 K. Mondal, B. Balasubramaniam, A. Gupta, A.A. Lahcen, and M. Kwiatkowski //J. Nanotechnol, 2019, 10-12 (2019).

12 M. Kwiatkowski, A. Policicchio, M. Seredych, and T.J. Bandosz, Carbon N. Y., 98, 250-257 (2016).

13 T.H. Ting, R.P. Yu, and Y.N. Jau, Mater. Chem. Phys., 126, 364-370 (2011).

14 A. Houbi, A.A. Zharmenov, Y. Atassi, Z.T.Bagasharova, S. Mirzalieva, K.Kadyrakunov, J Magn Magn Mater., 529 167839 (2021).

15 L.T.Q. Anh and N. Van Dan, Appl. Phys. A Mater. Sci. Process., 126, 1-6 (2020).

16 V.K. Chakradhary and M.J. Akhtar, 2017 IEEE Asia Pacific Microwave Conference (APMC), 678-681 (2017).

17 A.M. El Nahrawy, H.S. El-Deen, A.A. Soliman, and W.M.M. Mosa, Egypt. J. Chem., 62, 925-957 (2019).

18 E. Hu, X. Hu, T. Liu, L. Fang, K.D. Dearn, and H. Xu, Wear, 304, 152-161 (2013).

19 S.B. Kondawar and A.I. Nandapure, J. Chinese Adv. Mater. Soc., 2, 186-198 (2014).

20 S.J. Figueroa Ramírez and M. Miranda-Hernánde, Int. J. Electrochem. Sci., 7, 150-166 (2012).

21 S.Y. Kim, S.H. Kwon, Y.D. Liu, J.S. Lee, C.Y. You, and H.J. Choi, J. Mater. Sci., 49, 1345-1352 (2014).

22 P. Verma, T. Bansala, S.S. Chauhan, D. Kumar, S. Deveci, and S. Kumar/ J. Mater. Sci., 56, 11769 (2021).

23 M. Bayat, H. Yang, F.K. Ko, D. Michelson, and A. Mei, Polymer (Guildf), 55, 936-943 (2014).

24 Y.K. Hong, C.Y. Lee, C.K. Jeong, D.E. Lee, K. Kim, and J. Joo, Rev. Sci. Instrum., 74, 1098 (2003).

25 S. Wang, Q. Jiao, Q. Shi, H. Zhu, T. Feng, Q. Lu, C. Feng, H. Li, D. Shi, and Y. Zhao, Ceram. Int., 46, 1002-1010 (2020).

26 R. Shu, J. Zhang, C. Guo, Y. Wu, Z. Wan, J. Shi, Y. Liu, and M. Zheng, Chem. Eng. J., 384 123266 (2020).

27 R. Jaiswal, K. Agarwal, R. Kumar, R. Kumar, K. Mukhopadhyay, and N.E. Prasad, Soft Matter, 16, 6643 (2020).

28 N.N. Ali, Y. Atassi, A. Salloum, A. Malki, M. Jafarian, and R.K.B. Almarjeh, J. Mater. Sci. Mater. Electron., 30, 6876-6887 (2019).